Saudi Pharmaceutical Journal 30 (2022) 863–873

Contents lists available at ScienceDirect

Saudi Pharmaceutical Journal

journal homepage: www.sciencedirect.com

Original article

Empagliflozin attenuates neurodegeneration through antioxidant, anti-inflammatory, and modulation of α-synuclein and Parkin levels in rotenone-induced Parkinson's disease in rats

Sanaa Ahmed [a], Mahmoud M. El-Sayed [b], Mohamed A. Kandeil [c], Marwa M. Khalaf [b,*]

[a] Pharmacology Department, Faculty of Medicine, Sohag University, Sohag 82524, Egypt
[b] Pharmacology & Toxicology Department, Faculty of Pharmacy, Beni-Suef University, Beni-Suef 62514, Egypt
[c] Biochemistry Department, Faculty of Veterinary Medicine, Beni-Suef University, Beni-Suef 62514, Egypt

ARTICLE INFO

Article history:
Received 23 November 2021
Accepted 10 March 2022
Available online 16 March 2022

Keywords:
Parkinsonism
Neuroprotection
SGLT-2 inhibitors
Neurodegeneration
Rotenone
α-synuclein

ABSTRACT

Sodium-glucose co-transporter 2 (SGLT 2) inhibitors are a relatively new antidiabetic drug with antioxidant and anti-inflammatory properties. Therefore, this study aimed to investigate whether SGLT 2 inhibitors have a neuroprotective effect in PD. Twenty-four Wistar rats were randomized into four groups. The first one (control group) received dimethyl sulfoxide (DMSO) as a vehicle (0.2 mL/48 hr, S.C). The second group (positive control) received rotenone (ROT) (2.5 mg/kg/48 hr, S.C) for 20 successive days, whereas the third and fourth groups received empagliflozin (EMP) (1 and 2 mg/kg/day, orally), respectively. The two groups received rotenone (2.5 mg/kg/48 hr S.C) concomitantly with EMP for another 20 days on the fifth day. By the end of the experimental period, behavioral examinations were done. Subsequently, rats were sacrificed, blood samples and brain tissues were collected for analysis. ROT significantly elevated oxidative stress and proinflammatory markers as well as α-synuclein. However, dopamine (DP), antioxidants, tyrosine hydroxylase (TH), and Parkin were significantly decreased. Groups of (EMP + ROT) significantly maintained oxidative stress and inflammatory markers elevation, maintained α-synuclein and Parkin levels, and elevated TH activity and dopamine level. In both low and high doses, EMP produced a neuroprotective effect against the PD rat model, with the high dose inducing a more significant effect.

1. Introduction

Parkinson's disease (PD) is the second most public neurodegenerative disease affecting central and peripheral nervous systems. The neurodegeneration process appears as a consequence of dopaminergic neurons damage in substantia nigra, inducing a marked decline in the striatum levels of dopamine (DP) (Acar et al., 2019). Although most research has focused on the basal ganglia in Parkinson's disease pathology, some evidence suggests that the cerebellum also contributes to PD related to motor and cognitive decline through the loss of Purkinje cells neurons, which were present in the cerebellum and were responsible for regulating and coordinating movement via releasing of GABA neurotransmitter (Hasan et al., 2020a; Piras et al., 2021). Globally, PD affects 1% of people over the age of 60 and 5% of people over the age of 85 (Balestrassi and Silva, 2021). In Egypt, approximately 2500–2750 per lakh of the population ≥ 50 years suffer from PD attributed

Abbreviations: CP, Ceruloplasmin; DP, Dopamine; DMSO, Dimethyl sulphoxide; DOPAC, Dihydrophenyl acetic acid; DOPAL, Dihydroxyphenylacetaldehyde; EMP, Empagliflozin; GABA, γ-Aminobutyric acid; GSH, Reduced glutathione; IL-1β, Interlukine 1β; MAO, Monoamine oxidase; MDA, Malondialdehyde; NO, Nitric oxide; PD, Parkinson's disease; ROS, Reactive oxygen species; ROT, Rotenone; SGLT 2, Sodium glucose co-transporter 2; SOD, Superoxide dismutase; TNF-α, Tumor necrosis factor–α; TH, Tyrosine hydroxylase; α–syn, Alpha-synuclien.

* Corresponding author.
E-mail addresses: sanaa_ahmed@med.sohag.edu.eg (S. Ahmed), marwa.khalaf@-pharm.bsu.edu.eg (M.M. Khalaf).

Peer review under responsibility of King Saud University.

Production and hosting by Elsevier

https://doi.org/10.1016/j.jsps.2022.03.005
1319-0164/

to the exposure of a high percentage of the workforce to pesticides in agriculture (Rösler et al., 2018).

The main feature of Parkinson's disease (PD) is the accumulation of misfolded alpha -synuclein (α-syn) protein aggregates, which results in the formation of Lewy's bodies (Recasens et al., 2014). In addition, mutations in Parkin and Dj-1 genes may be involved in the onset of PD. Parkin mutation causes mitochondrial dysfunction, which is considered a central contributor in PD pathogenesis, while Dj-1 mutation produces a defect in the protective role of antioxidants (Dodson and Guo, 2007). In PD, oxidative stress is thought to be the definite fundamental pathway that initiates the dysfunction of neurons cells (Hwang, 2013). The substantia nigra of patients with PD demonstrated an elevation in the oxidation rate of proteins, lipids, and DNA (Nakabeppu et al., 2007).

When there is an imbalance between the generation of reactive oxygen species (ROS) and the cellular defense antioxidant system, oxidative stress occurs. Dopaminergic neurons become exclusively more susceptible to oxidative stress due to the presence of some ROS-generating enzymes such as monoamine oxidase (MAO) and tyrosine hydroxylase (TH) (Hwang, 2013; Wei et al., 2018). Inflammation significantly contributes to the initiation and progression of neurodegeneration. It is primarily produced due to microglial activation, where it secretes many proinflammatory cytokines and neurotoxic substances (Goldstein, 2020). Moreover, insulin resistance may be associated with PD contributing to the disease progression and acceleration (Kalampokini et al., 2019).

One of the newest hypotheses for PD is the accumulation of toxic intermediate product 3,4-dihydroxyphenyl acetaldehyde (DOPAL) produced from MAO-catalyzed dopamine oxidation. DOPAL can interact with α-syn and induce its oligomerization process forming the major component of Lewy's bodies (Goldstein, 2020).

Rotenone (ROT) is a natural pesticide extracted from Leguminosae plants. Administration of ROT results in a selective and potent complex-I inhibition which is a feature of idiopathic PD. In addition, ROT administration leads to selective dopaminergic neurodegeneration, oxidative stress, α-syn accumulation, and microglial activation (Anusha et al., 2017).

Like metformin and liraglutide, many hypoglycemic agents exhibit antioxidant and anti-inflammatory potential at the central level (Oliveira et al., 2016; Fanget al., 2012). Sodium-glucose cotransporter 2 (SGLT 2) is responsible for the reabsorption of more than 90% of the total renal-filtered glucose expressed in proximal tubules. Empagliflozin (EMP) is an SGLT 2 inhibitor recently approved as an antidiabetic drug due to its additional antioxidant and anti-inflammatory benefits (Li et al., 2019; Lai et al., 2020).

It is well known that all medications used in the treatment of PD are symptomatic, and their efficacy diminishes with time (Mao et al., 2020). Therefore, one of the best strategies in treating PD is to search for new effective drugs to prevent neuronal death and slow down the PD disease progression. Therefore, the current study attemoted to investigate the potential protective effect of EMP as a new SGLT 2 inhibitor against rotenone-induced PD in rats.

2. Material and methods

2.1. Animals

Twenty-four male albino Wistar rats 180–220 gm in weight were used in this investigation. Animals were obtained from the animal house, Faculty of Medicine, Sohag University, Egypt. Then, they were kept under suitable environmental conditions (temperature around 25 ± 2 °C and 12 h light/dark). Rats were left one week before starting the experiment for accommodation. Throughout the experiment, animals were nourished with standard pellet chew and had free access to tap water *ad libitum*. This experimental protocol was approved (Approval No. 021-160) according to the Medical Research Ethics Committee guidelines, Faculty of Pharmacy, Beni-Suef University, Egypt, under the recommendations of the EU strategies 2010/63/EU for experimental animals.

2.2. Drugs and chemicals

ROT and interleukin-1B (IL-1B) ELISA kits were purchased from Sigma Aldrich (St. Louis, MO, USA), while EMP (Jardiance) was obtained from Boehringer Ingelheim (Germany). DMSO and sunflower oil were purchased from El-Nasr chemical company (Cairo, Egypt). Glutathione (GSH), superoxide dismutase (SOD), nitric oxide (NO), and blood glucose kits were acquired from the Biodiagnostic Company (Giza, Egypt). Malondialdehyde (MDA) kit was obtained from Eagle Biosciences, Inc. (Boston, USA). Ceruloplasmin (CP) and DP ELISA kits were purchased from Indomedix Egypt (Cairo, Egypt). Tumor necrosis factor-alpha (TNF-α), dihydroxyphenylacetic acid (DOPAC), and MAO-B ELISA kits were gained from RayBiotec, (GA, USA), SunLong Biotech Company (China), and MyBioSource, Inc. (San Diego, USA), respectively. Fast Cast acrylamide kit (SDS-PAGE) and ReadyPrep TM protein abstraction kit (total protein) were supplied by Bio-Rad Laboratories Inc. Bradford protein analysis kit (SK3041) for protein investigation quantitatively was provided by Bio basic Inc (Markham Ontario L3R 8T4 Canada). Rabbit Anti-TH antibody Neuronal Marker (ab112) and immunohistochemical detection system were obtained from Lab vision Neomarker (USA).

2.3. Study design

Rats were randomized into four groups (six rats each). The first cohort (normal control) received only vehicle (1 mL DMSO diluted in sunflower oil to 50 mL) given in a dose of (0.2 mL/48 hr S.C). The second group (positive control) received ROT (2.5 mL/kg/48 hr S.C) for 20 days (Hassanzadeh et al., 2014). ROT (2.5 mg/mL) was prepared by dissolving 12.5 mg ROT in a 5 mL vehicle (DMSO + sunflower oil). The third and fourth groups received EMP 1 and 2 mg/kg/day orally, respectively (Han et al., 2017). On the fifth day of EMP treatment, animals received ROT (2.5 mg/kg/48 hr S.C) concomitant with EMP for additional 20 days. After finishing the experiment, the behavioral tests were performed, and then rats were sacrificed, blood samples were collected, and brains were removed for assay.

2.4. Induction of PD

For PD induction, rats were injected with ROT (2.5 mg/kg/48 hr S.C) for 20 days (Hassanzadeh et al., 2014). The rotarod test was performed every 48 hr to ensure that induction was done.

2.5. Behavioral investigations

2.5.1. Open field test

In order to assess locomotor performance, open-field assessment was applied. The open field gadget is a square field manufactured of wood (100 × 100 × 40 cm) with a ground divided into 25 identical-size squares with webs. After being placed in the center of the apparatus, a video camera was fixed on the top of the box to record animal ambulation (number of quadrangles overpassed by the animals with its all paws in one minute) (Neto et al., 2013).

2.5.2. Rotarod test

Rotarod test is a behavioral test used to assess motor coordination in the PD rat model. Before starting the test, animals were allowed to train for three successive days on apparatus until reach-

ing stable performance. Animals were placed on a circling rod with 15 rpm speed. Each rat could stopover was listed as the latency period to drop. The test was repeated three times for each rat, with a 10-minute rest interval in between to avoid lethargy and tension, and the mean was calculated for each animal (Voss et al., 2003).

2.6. Sample preparation

2.6.1. Blood collection and serum separation

After the end of the experiment, blood samples were collected from all animals under anesthesia from the *retro*-orbital venous plexus in sterile tubes. Samples were then centrifuged at 2000 r.p.m. for 10 min for separation of clear serum to be kept at −20 °C until the analysis time. The serum was used for the estimation of blood glucose levels.

2.6.2. Preparation of brain tissue homogenate

The brain tissue containing striatum, substantia nigra, and cerebellum were quickly removed and cleaned using normal cold saline and weighed. One portion of brain tissue was homogenized in 10 mL cold phosphate buffer (100 mM potassium phosphate, PH 7.0, containing 2 mM EDTA) per gram brain tissue then centrifuged at 4000 r.p.m. for 15 min at 4 °C. Finally, the clear supernatant was separated for the biochemical assessment of the brain content of GSH, SOD, MDA, NO, IL-1β, TNF-α, MAO-B, CP**,** DP, and its metabolites. The second part was lysed in RIPA buffer for western blotting estimation of α-syn and Parkin protein expression. The third part of the tissue containing substantia nigra was immersed in liquid nitrogen and preserved at –80 °C for immunohistochemical investigation of TH enzyme activity. The remaining part, which contains the cerebellum, was incubated in formalin until the histopathological analysis.

2.7. Determination of blood glucose level

Blood glucose level was measured colorimetrically using NO GL 13 20 kit acquired from Biodiagnostic Co, Giza, Egypt. The hydrogen peroxide produced from glucose by glucose oxidase action at pH 7 is determined by the peroxidase oxidative coupling of N, N-diethylaniline with 4-amino-antipyrine. A 20-μl sample of blood serum reacted with a colorimetric kit containing (phosphate buffer, phenol, 4-amino-antipyrin and glucose oxidase) for 10 min at room temperature and pH 7. A red violet color was formed and was measured at 553 nm (Kabasakalian et al., 1974).

2.8. Determination of antioxidant and oxidative stress biomarkers in brain tissue

GSH concentration in brain tissue homogenate was measured colorimetrically using NO GR 25 11 kit obtained from Biodiagnostic Co., Giza, Egypt. The procedure was performed according to the manufacturers' instructions provided. GSH estimation depends on the reduction of Ellman's reagent [5,5′-dithiobis (2-nitrobenzoic acid)] by glutathione to yield a yellow-colored product (Ellman, 1959). The absorbance of this reduced chromogen was measured at 405 nm and it was directly related to GSH concentration.

SOD activity in brain tissue homogenate was also determined colorimetrically, using NO SD 25 21 kit purchased from Biodiagnostic Co., Giza, Egypt. The procedure was performed according to the manufacturers' instructions provided. Determination of SOD is based on the ability of this enzyme to inhibit phenazin methosulphate-mediated reduction of nitroblue tetrazolium dye (Marklund and Marklund, 1974).

Lipid peroxides were evaluated using a kit purchased from Eagle bioscince Co. with Catalog Number: LIP39-*K*01. The provided procedure of the manufacturer was followed. The method is based on the response of a chromogenic reagent, N-methyl-2- phenylindole, to malondialdehyde (MDA) at 45 °C. One particle of MDA reacts with 2 particles of chromogenic reagent to produce a constant chromophore with maximal absorbance at 586 nm (Uchiyama and Mihara, 1978).

NO was evaluated using a kit: NO 25 33 from Biodiagnostic Co., Giza, Egypt according to the procedure provided by the manufacturer. It can be measured as the final product of NO in vivo which is nitrite (NO^{2-}). Colorimetric nitrite determination depends on addition of Griess reagent which convert nitrite into deep purple azo compound. The photoabsorbance of this compound accurately determines nitrite (Montgomery and Dymock, 1961).

2.9. Determination of IL-1β, TNF-α, DP, and DOPAC contents as well as MAO-B activity in brain tissue

The brain content of IL-1β, TNF-α, DP, and DOPAC, and the brain activity of MAO-B were measured by using the monoclonal double-antibody sandwich ELISA method as described by the manufacturers' prescriptions. Concentrations were measured using 2600 microplate State Fax reader (Awareness Technologies, Palm City, USA). This assay employs antibodies specific for Rat IL-1β, TNF-α, DP, DOPAC or MAO-B, respectively coated on a specific provided well plate. Standards and samples are pipetted into the wells and IL-1β, TNF-α, DP, DOPAC or MAO-B present in the sample is bounded to the wells by the immobilized antibody. The wells were washed and biotinylated antiRat IL-1β, TNF-α, DP, DOPAC or MAO-B antibody is added. After washing of any unbound biotinylated antibody, HRP conjugated streptavidin is pipetted to the wells. The wells are again washed and tetramethylebenzidine (TMB) substrate solution is added to the wells and color develops in proportion to the amounts of IL-1β, TNF-α, DP, DOPAC or NAO-B bound. The Stop Solution changes the color from blue to yellow, and the intensity of the color is measured at 450 nm (Finch et al., 1995; Laczko et al., 2020; Chakraborty and Diwan, 2019).

2.10. Determination of ceruloplasmin (CP) content in brain tissue

According to the producer's directions, CP was estimated using the competitive ELISA technique (Saraf et al., 2016). Samples were added to Horseradish Peroxidase (HRP) conjugated antibody preparation specific for CP. The absorbance was measured using a 2600 microplate State Fax reader (Awareness Technologies, Palm City, USA).

2.11. Western blotting analysis of α-syn and Parkin proteins

The brain tissue was homogenized in RIPA lysis buffer and centrifuged at 4 °C for 20 min at 12,000 rpm, and then the supernatant was taken. The total concentration of protein was assessed by the Bradford protein assay kit (**SK3041)** (Bio basic Inc Canada) (Gilda and Gomes, 2013). 20 ug/mL protein concentration of each sample was overloaded with an equivalent volume of Laemmli buffer (4% SDS, 10% 2-mercaptoethanol, 20% glycerol, 0.004% bromophenol blue, and 0.125 M Tris HCL. These mixtures were incubated at 95 °C for 5 min to confirm protein denaturation. Samples with an equal amount of proteins were parted with 10% SDS-PAGE. Polyacrylamide gels were done using TGX Stain-free. The SDS-PAGE TGX Stain-Free Fast Cast was prepared following the producer's instructions. The gel was collected in a transfer PVDF film blocked in tris-buffered saline (3% bovine serum albumin and Tween 20) for one hour at temperature. Afterward, the blot was run for 7 min at 25 V to allow protein bands to transfer from the gel to film using BioRad Trans-Blot Turbo. The film was incubated with an anti-α-syn and anti-Parkin antibody. The objective proteins were

identified by ChemidocTM XRS + system with Image Lab software (Bio-Rad, USA), and band intensity was quantified by the Image Lab program (Peferoen et al., 1982).

2.12. Immunohistochemical study of TH enzyme

After deparaffinization, tissue slices were gained by xylene overnight then hydrated in alleviated concentrations of alcohol 100, 90, 70, and 50% for 5 min each. Antigen retrieval was carried out by warming slides in citrate buffer (pH 6) in the microwave for 5 min and washed twice in PBS for 20 min. 3% hydrogen peroxide solution was used for 10 min for blocking the activity of endogenous peroxide, then washed twice in PBS (pH 7.2) for 5 min each. The sections were treated for one hour. in a moisture compartment with rabbit polyclonal antibody against TH (Lab vision Neomarker USA) branded as a dark brown reaction inside the cytoplasm. The slides were washed in PBS, and biotinylated secondary antibody (Universal Multilink) was applied for 10 min and washed twice. The bound antibodies were established using streptavidin peroxidase 2 drops on the sections for 30 min and washed for 5 min, then exposed for 10 min to freshly prepared diaminobenzidine (DAB) and chromogen. After the appearance of the brown color, the slides were instantly washed in tap water. The sections were stained with hematoxylin for the detection of tissue architecture. The slides were dehydrated, and the cover slipped using Flotex permanent mountain media (Renshaw, 2006).

2.13. Histopathological examination of cerebellum

Following fixation in neutral buffered formalin and dehydrated in ascending grades of alcohol, tissues were fixed in Paraffin; slices of 5 µm thickness were established using Micro-Teck microtome (Germany). Subsequently, slides were stained in Erlich's hematoxylin for 5 min and blued in tap water for 3 min after they were stained in 1% aqueous eosin solution for 1 min then washed in the water finally dehydrated in alcohol and cleared in xylol then studied by an Olympus (model CX21) Japan, light microscope (Suvarna et al., 2018).

2.14. Statistical analysis

Data were presented as mean ± SEM, and quantitative variables were compared using a one-way ANOVA using (IBM-SPSS version 22.0) software package, followed by Tukey Kramer's post hoc test for multiple comparisons. The level of significance was determined at a *P*-value $\leq$ 0.05.

3. Results

3.1. Effect of EMP on blood glucose level

Regarding blood glucose level, no significant difference was observed between the different groups at $p < 0.05$ as shown in Fig. 1.

3.2. Behavioral study

The results of the open field and rotarod tests revealed that ROT had a significant reduction in both locomotor activity and motor coordination compared to the control group. The reduction in these activities confirmed PD induction in the ROT group. However, when EMP was administered concurrently with ROT in both low and high doses, it significantly improved locomotor activity and motor coordination compared to the ROT group. When the results of 1 and 2 mg/kg EMP doses were compared, it was discovered that

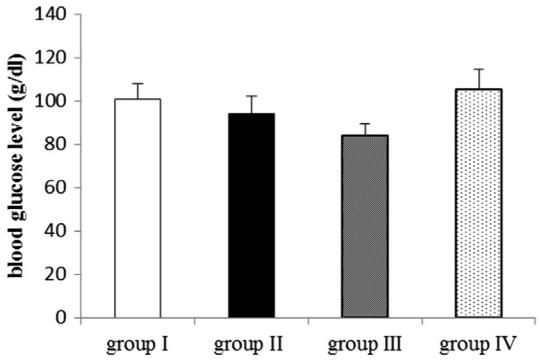

Fig. 1. Effect of EMP on blood glucose level in ROT-induced PD in male Wistar rats. Data were presented as mean ± SEM n = 6. group I = control group. group II = ROT group. group III = EMP1mg + ROT group. group IV = EMP2mg + ROT group.

the dose of 2 mg/kg EMP showed a significant improvement in motor coordination than 1 mg/kg dose, while no significant difference between the two doses was observed regarding the locomotor activity (Fig. 2 **A and B**).

3.3. Effect of EMP on the brain content of antioxidant and oxidative stress biomarkers

As revealed in Table 1, ROT administration showed a significant reduction in the brain GSH content and SOD enzyme activity with a significant promotion in the brain content of MDA and NO com-

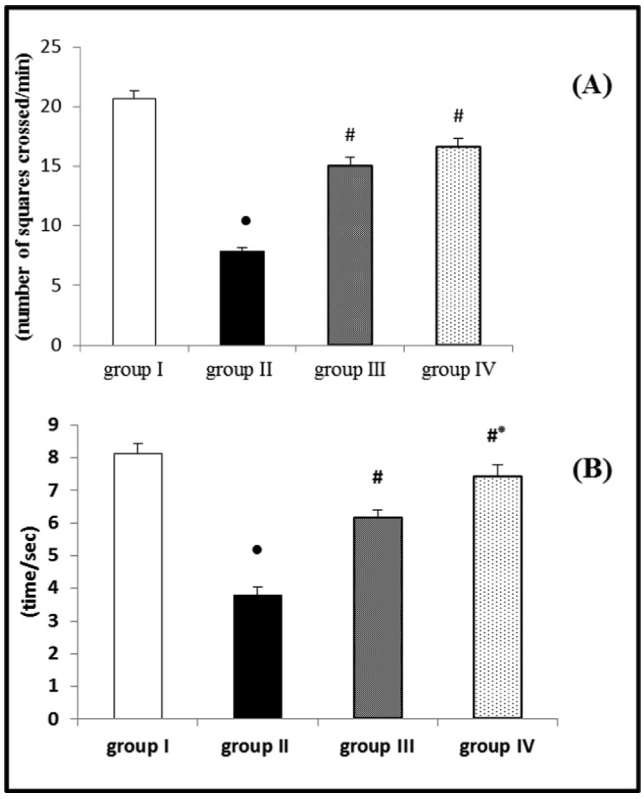

Fig. 2. Effect of EMP on (A) locomotor activity determined by open field test and (B) motor coordination determined by rotarod test in ROT-induced PD in male Wistar rats. Data were presented as mean ± SEM n = 6. ● Significantly different when compared to the control group at $p < 0.05$. # Significantly different when compared to ROT group at $p < 0.05$. * Significantly different when compared to EMP (low dose) group at $p < 0.05$. group I = control group. group II = ROT group. group III = EMP1mg + ROT group. group IV = EMP2mg + ROT group.

Table 1
Effect of EMP on the brain content of antioxidant and oxidative stress biomarkers in ROT-induced PD in male Wistar rats.

Parameters	Control	ROT	EMP(1 mg/kg) + ROT	EMP(2 mg/kg) + ROT
GSH)mg/g tissue)	564 ± 42.42	144 ± 12.92●	426 ± 23.42#	568 ± 18.93#*
SOD (U/g tissue)	750 ± 43.67	266.5 ± 18.20●	605 ± 24.42#	748 ± 20.73#*
MDA (nmol/g tissue)	0.3113 ± 0.02	3.17 ± 0.02●	0.76 ± 0.03#	0.367 ± 0.01#*
NO μmol/g tissue))	2.48 ± 0.16	9.22 ± 0.74●	4.39 ± 0.07#	3.56 ± 0.09#*

Data were presented as mean ± SEM n = 6.
● Significantly different when compared to the control group at $p < 0.05$.
Significantly different when compared to ROT group at $p < 0.05$.
* Significantly different when compared to EMP (low dose) group at $p < 0.05$.
EMP = empagliflozin ROT = rotenone GSH = glutathione.
SOD = superoxide dismutase MDA = malonaldehyde NO = nitric oxide.

pared to the control group. In contrast, EMP administration either in 1 mg or 2 mg concurrent with ROT led to a significant upturn in GSH content and SOD activity with a significant decline in MDA and NO's brain content compared to the ROT group. Besides, administration of EMP in high doses induced significant improvement in the previously measured parameters compared to low doses.

3.4. Effect of EMP on the brain content of proinflammatory cytokines (IL-1B and TNF-α)

Administration of ROT caused a significant upsurge in the brain content of IL-1B and TNF-α versus the control group, while administration of EMP either in a dose of 1 or 2 mg/kg concurrent with ROT led to a significant fixing in these parameters versus the ROT group. In comparison between the two EMP doses, there was more significant improvement with the high dose than the low dose, as depicted in (Table 2).

3.5. Effect of EMP on the brain content of DP and DOPAC

Administration of ROT led to a significant reduction in DP and DOPAC content in the brain tissue homogenate compared to the control group. On the contrary, administration of EMP either in a dose of 1 or 2 mg/kg concurrent with ROT resulted in a significant saving in DP and DOPAC contents compared to the ROT group. Administration of the high dose of EMP produced a significant decrease in these parameters compared to the low dose, as demonstrated in (Fig. 3 **A and B**).

3.6. Effect of EMP on the brain monoamine oxidase-B (MAO-B) activity and ceruloplasmin (CP) content in brain tissue

ROT administration resulted in a significant increase in MAO-B activity and a significant decrease in CP content compared to the control group, as displayed in (Table 3). However, administering EMP at a dose of 1 or 2 mg/kg concurrently with ROT resulted in a significant reduction in MAO-B activity and a significant increase in CP content compared to the ROT group. When comparing the two EMP doses, the high dose resulted in more significant improvement than the low dose.

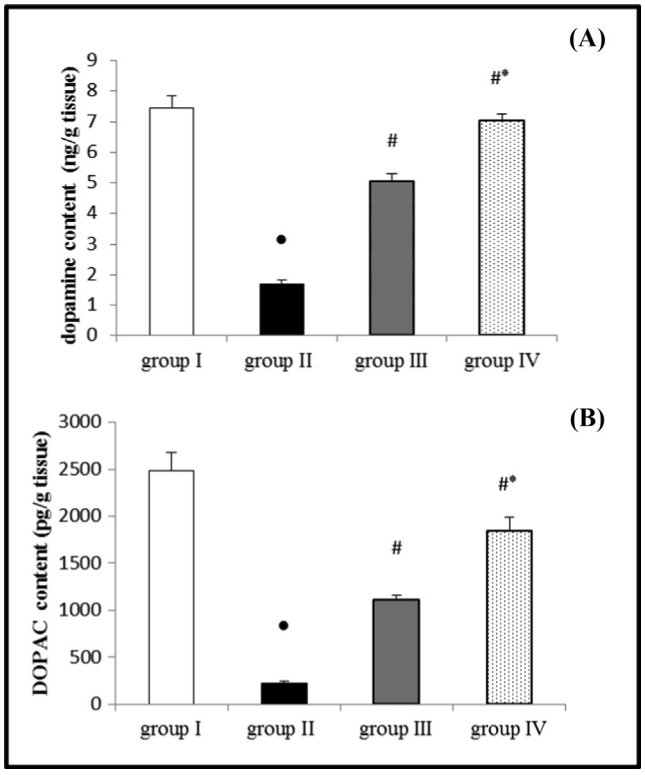

Fig. 3. Effect of EMP on the brain content of (A) dopamine and (B) DOPAC in ROT-induced PD in male Wistar rats. Data were presented as mean ± SEM n = 6. ● Significantly different when compared to the control group at $p < 0.05$. # Significantly different when compared to ROT group at $p < 0.05$. * Significantly different when compared to EMP (low dose) group at $p < 0.05$. group I = control group. group II = ROT group. group III = EMP1mg + ROT group. group IV = EMP2mg + ROT group. DOPAC = dihydrophenyl acetic acid.

Table 2
Effect of EMP on the brain content of proinflammatory cytokines in ROT-induced PD in male Wistar rats.

Parameters	Control	ROT	EMP(1 mg/kg) + ROT	EMP(2 mg/kg) + ROT
IL-1B (ng/g tissue)	491.8 ± 4.74	8352 ± 462.90●	2066 ± 176.06#	579.50 ± 15.45#*
TNF-α (ng/g tissue)	321.2 ± 5.93	4755 ± 298.30●	2152 ± 139.00#	578 ± 22.65#*

Data were presented as mean ± SEM n = 6.
● Significantly different when compared to the control group at $p < 0.05$.
Significantly different when compared to ROT group at $p < 0.05$.
* Significantly different when compared to EMP (low dose) group at $p < 0.05$.
EMP = empagliflozin ROT = rotenone.
IL-1β = interlukin- 1β TNF-α = tumor necrosis factor –α.

Table 3
Effect of EMP on the brain MAO-B activity and CP content in ROT-induced PD in male Wistar rats.

Parameters	Control	ROT	EMP(1 mg/kg) + ROT	EMP(2 mg/kg) + ROT
MAO-B U/mg tissue))	31.32 ± 1.73	156.5 ± 5.20●	66.48 ± 4.88#	42.23 ± 3.21#*
CP ng/g tissue))	320.8 ± 18.35	74.33 ± 3.24●	221.33 ± 18.23#	307.33 ± 22.04#*

Data were presented as mean ± SEM n = 6.
● Significantly different when compared to the control group at $p < 0.05$.
Significantly different when compared to ROT group at $p < 0.05$.
* Significantly different when compared to EMP (low dose) group at $p < 0.05$.
EMP = empagliflozin ROT = rotenone.
MAO-B = monoamineoxidase-B CP = ceruloplasmin.

3.7. Effect of EMP on α-syn and Parkin protein expression

ROT administration resulted in a significant increase in total -syn, but a significant decrease in Parkin protein expression compared to the control group. However, when compared to the ROT group, groups that received EMP at a dose of 1 or 2 mg/kg concurrently with ROT showed a significant restriction in α-syn and a significant saving in Parkin protein expression. As depicted in Fig. 4 high dose EMP caused a significant change in α-syn and Parkin protein expression than low dose, as demonstrated in **Fig. (4 A, B and, C).**

3.8. Effect of EMP administration on tyrosine hydroxylase (TH) immunohistochemistry

The immunohistochemical analysis of substantia nigra in the control group showed positive staining of TH as a brown cytoplasmic reaction (Fig. 5 A). (ROT group): revealed a marked decrease in TH immunoreactivity compared to the control group (Fig. 5 B). Pronounced preservation was observed in TH immunoreactivity in the EMP + ROT treated groups and there is a dose-dependent improvement compared to the ROT group. (Fig. 5 **C and D**). These photomicrographs correlate with the values of mean A% displayed in (Fig. 6).

3.9. Effect of EMP on histopathological examination for the cerebellum

As demonstrated in Fig. 7**,** histological examination of the cerebellar tissue of the control group revealed normal histological structure. With regard to the ROT group, it demonstrated a decreased number of Purkinje cells with shrunken darkly stained nuclei and dilated perineural space. Co-administration of EMP1 + ROT; cerebellar tissue showed many nerve fibers and dendrites with few numbers of Purkinje cells with dilated perineural space. Co-administration EMP2 + ROT, cerebellar cortex showed restoration of the normal histological structure.

4. Discussion

This study was directed to evaluate the potential neuroprotective effect of EMP on rats model of ROT-induced PD. EMP is a selective inhibitor of $SGLT_2$ that reduces hyperglycemia in type 2 diabetic patients by inhibiting glucose renal reabsorption, leading to increased glucose renal excretion (Zinman et al., 2015). Glucose level regulation in the brain occurred by SGLTs may contribute to the expectation of EMP central neuroprotective effect (Yu et al., 2010).

Metformin is a common glucose-lowering drug that has been found to protect neurons in animal and cellular models by decreasing α-syn aggregation, preventing mitochondrial dysfunction, and giving antioxidant effects (Lin et al., 2021). Other antidiabetic medications with neuroprotective effects include a peroxisome proliferator-activated receptor-gamma (PPAR) agonists such as Pioglitazone, which can assist in reducing inflammation after a traumatic brain injury (Deng et al., 2020) or in a Parkinson's disease model caused by 6-hydroxydopamine (Machado et al., 2019). Furthermore, exendin-4, liraglutide, and lixisenatide are GLP-1RAs that raise striatal DP and TH protein levels in the 1-me thyl-4-phenyl-1,2,3,6-tetrahydropyridine animal model of PD (Liu et al., 2015).

The current study revealed that EMP did not produce hypoglycemia, as evidenced by the blood glucose level estimation. This result is consistent with a previous study which stated that EMP does not produce severe hypoglycemia either alone or in combination with other antidiabetic drugs (metformin, sulphonylurea, or Pioglitazone) except with insulin (Ndefo et al., 2015).

Open field test is a behavioral test used to assess locomotion activity in PD models. Changes in locomotion are used as an indicator for alterations in the neurological state (Kraeuter et al., 2019). In addition, the rotarod test is a popular method used to investigate motor coordination and equilibrium in PD models (Hung and Hsueh, 2021). Our study revealed that ROT administration to experimental animals produced deterioration of behavioral function (locomotor activity by 62% and motor coordination by 54.42%), which is in harmony with previous research (Zaitone et al., 2019). However, rats that received EMP concurrent with ROT showed improvement in these functions compared with the ROT group (locomotor activity by 91.5%, 112% and motor coordination by 66.22%, 100% in low and high doses, respectively). This finding is in line with previously published studies that proved that SGLT 2 inhibitor, EMP, enhances open field performance in ischemic stroke (Amin et al., 2020) and dapagliflozin which improves these functions in ROT induced PD (Arab et al., 2021).

Oxidative stress is an imbalance between ROS generation and antioxidant defense mechanisms. It is believed to be the definite underlying cause that leads to cellular dysfunction (Hwang, 2013; Wei et al., 2018). To assess oxidative state in this study, we measured GSH, MDA, NO content, and SOD activity in brain homogenate. Our study revealed that ROT produced significant deterioration in the levels of these parameters (lowering in GSH content and SOD activity by 74% and 64%, respectively, while MDA and NO content showed an elevation by 918% and 272%, respectively) where these results are consistent with results of "Kaur et al. (2011) and Alabi et al. (2019)". The finding can explain these effects that ROT is a high-affinity inhibitor of complex-I of mitochondrial electron transport chain leading to increased production of free radicals resulting in oxidative damage "Sherer et al. (2003) and Chen et al. (2008)". On the other hand, our study revealed that EMP intake produced significant improvement in these parameters (an increase in GSH by 196%, 294% and SOD by 127%, 180%, while a decrease in MDA by 76%, 88%, and NO by 52%, 61% was observed in low and high doses respectively) where our findings align with another study (Shin et al., 2016). The antioxidant effect of EMP may be due to stimulation of the nuclear factor erythroid 2 (Nrf2)- related factor 2 pathway (Hasan et al., 2020b). This pathway has antioxidant function due to its vital role

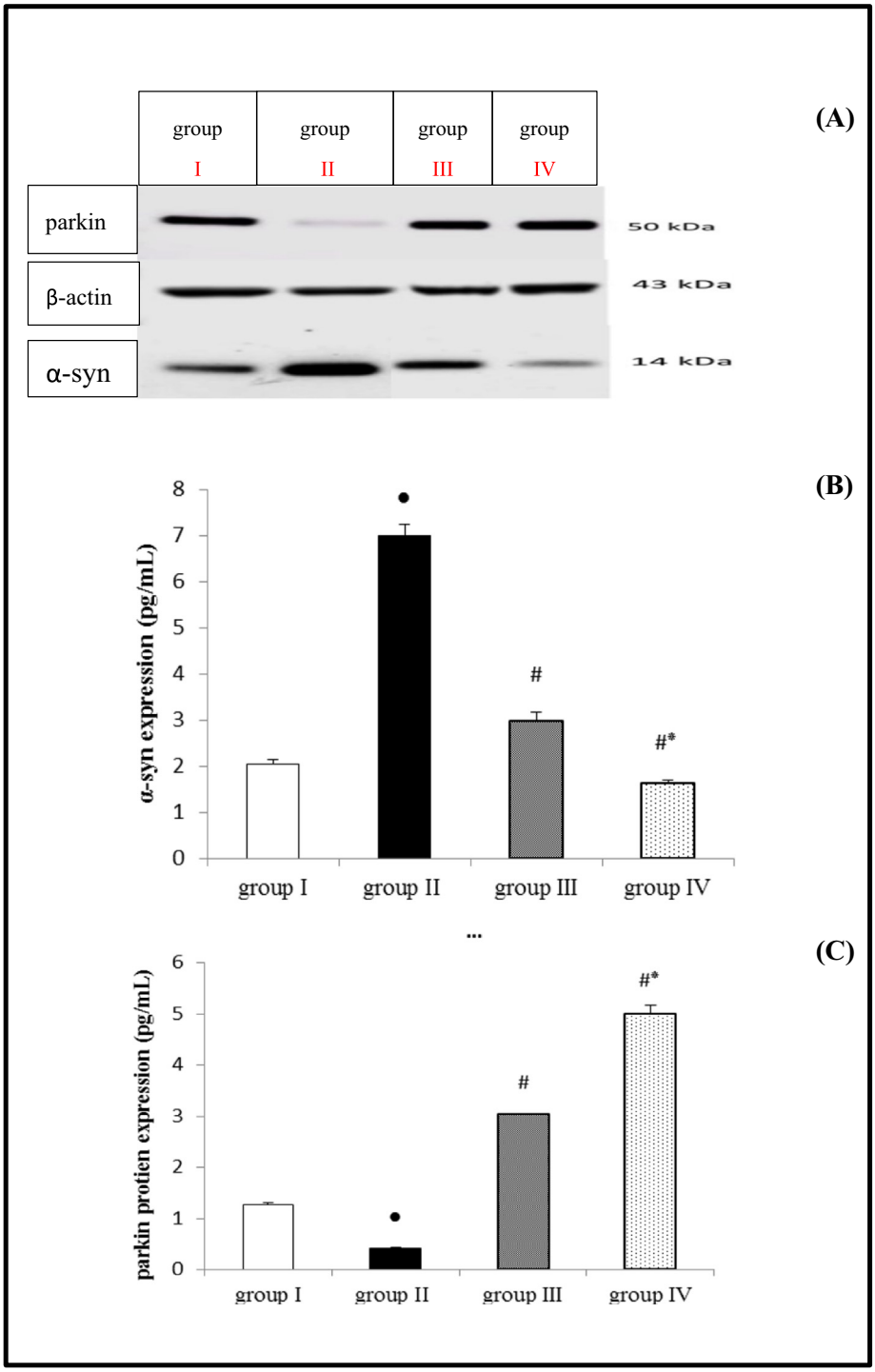

Fig. 4. Effect of EMP on α-syn and parkin protein expression in ROT-induced PD in male Wistar rats. Western blot bands (A), Densitometric quantitation of α-syn (B) and parkin (C) protein expressions. Data were presented as mean ± SEM n = 6. ● Significantly different when compared to the control group at $p < 0.05$. # Significantly different when compared to ROT group at $p < 0.05$. * Significantly different when compared to EMP (low dose) group at $p < 0.05$. group I = control group. group II = ROT group. group III = EMP1mg + ROT group. group IV = EMP2mg + ROT group. EMP = empagliflozin ROT = rotenone α-syn = α-synuclien.

in the expression of many genes for antioxidant enzymes such as SOD, glutathione-s-transferase (GST), NADPH quinone dehydrogenase-1 (NQO1). In addition, induction of this pathway was found to protect against cellular apoptosis (Ahmed and Mohammed, 2021).

ROT was previously reported to exert severe inflammatory potential that can be explained by its activation of NF-KB, which results in inflammatory cytokines elevation in microglia (Abdelsalam and Safar, 2015). IL-1β and TNF-α are neuroinflammatory markers produced due to ROT-activated microglia and/or as a response to α-syn aggregation (Hoffmann et al., 2016). These cytokines can trigger and extend neuroinflammation, resulting in blocking the induction of brain-derived neurotrophic factor (BDNF), an essential protein for dopaminergic neurons development and survival (Zhou et al., 2019). In our findings, ROT administration resulted in an increase in proinflammatory biomarkers IL-

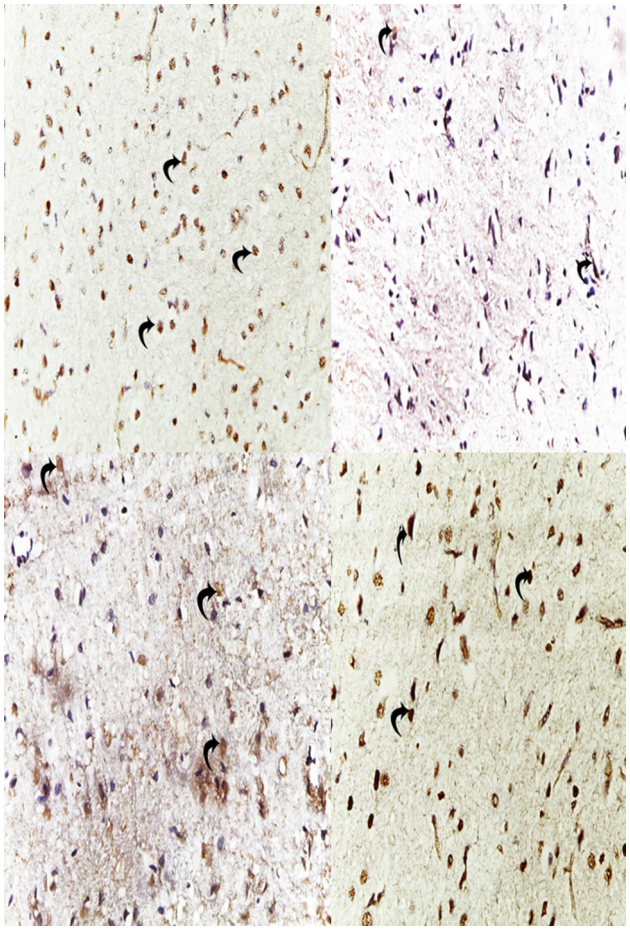

Fig. 5. (A) Immunohistochemical staining of striatal TH expression of the control group (400 X) showing the positive immune reaction of TH. **(B):** the ROT group revealed almost negligible immune reaction compared to the control group. **(C and D): EMP treated groups** showed restoration of staining of TH compared to the ROT group with a dose-dependent effect.

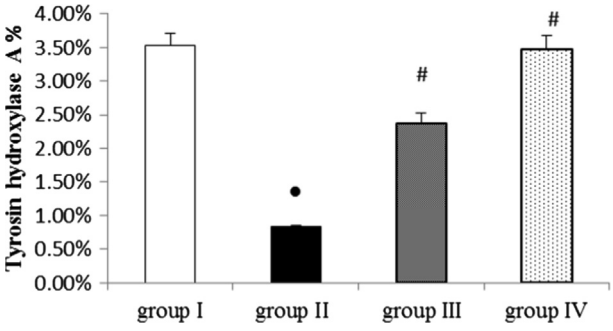

Fig. 6. Quantitative image analysis for TH immunohistochemical staining presented as mean area% (A%). Data were presented as mean ± SEM n = 6. ● Significantly different when compared to the control group at $p < 0.05$. # Significantly different when compared to ROT group at $p < 0.05$. * Significantly different when compared to EMP (low dose) group at $p < 0.05$. group I = control group. group II = ROT group. group III = EMP1mg + ROT group. group IV = EMP2mg + ROT group.

1B and TNF-α by more than ten times for each, which is consistent with (Mansour et al., 2018), while EMP + ROT administration resulted in significant restriction in IL-1β by 75%, 93% and 55%, 88% for TNF-α after low and high doses administration, respectively, compared to ROT group which is consistent with (Jojima et al., 2016). The anti-inflammatory effect of EMP can be attributed to the diminished activity of NF-KB, which suppresses proinflammatory mediators TNF-α and IL-1β expression. In addition, this anti-inflammatory potential can be related to its antioxidant effect (Abdelhamid et al.,2020).

DP is metabolized enzymatically by MAO-B in the brain, giving rise to DOPAC, which is further reduced to homovanillic acid (Jenner and Olanow, 1996). It is well known that MAO-B has a pathological role in PD via some toxin activation and free radicals formation (Thakur and Nehru, 2013). Our results demonstrated that ROT significantly increased MAO-B activity by 400%, reducing DP and DOPAC concentrations by 77% and 90%, respectively. These results are the same as the previously mentioned findings (Jenner and Olanow, 1996). This finding can be explained by the ROT-induced C/EBPβ pathway, which upregulates both MAO-B and α-syn transcription. In addition, dopamine metabolism by MAO-B strongly activates the δ-secretase enzyme leading to a positive feedback circuit in dopaminergic neurodegeneration (Wu et al., 2021). On the other hand, the administration of EMP + ROT resulted in the significant preservation of these parameters.

CP, a ferroxidase enzyme, plays a vital role in iron metabolism. It converts ferrous (Fe^{2+}) to less-toxic ferric iron (Fe^{3+}) (Liu et al.,2019). Our study showed a significant decrease in the brain CP content in the ROT-treated group by 77%. This result agrees with (Hineno et al.,2011) who owed this to CP consumption in preventing the oxidation and subsequent neurodegeneration caused by ROT. However, EMP administration revealed significant enhancement in CP by 198% and 314% for low and high EMP doses, respectively, which can be attributed to its antioxidant effect (Sugizaki et al.,2017) and its ability to regulate the copper homeostasis, which acts as a cofactor for the antioxidant Cu/Zn-SOD enzymes activity (Montes et al., 2014).

Our result showed that ROT led to a significantly upregulated α-syn level by 239% compared to the control group, which agrees with (Li et al., 2020) and significantly down-regulated parkin protein by 67%, which is compatible with (Rahimmi et al.,2015), while EMP + ROT resulted in significant preservation in these protein levels. α-syn is a fundamental contributor in PD, which can initiate and potentiates the neurodegeneration process by many pathways; inhibition of autophagy, induction of mitochondrial dysfunction, and increased oxidative stress in addition to microglial activation causing neuroinflammation and an increase in proinflammatory cytokines (Segura-Aguilar, 2017).

However, the lack of Parkin protein promotes dopaminergic neurodegeneration by affecting the mitochondrial morphology and function with potential membrane reduction (Pinto et al., 2018). Moreover, Parkin overexpression is shown to reduce MAO expression leading to further reduction in ROS produced through MAO catalyzed dopamine oxidation (Jiang et al., 2006).

All previous results are supported by the immunohistochemical TH estimation in substantia nigra, which referred to its decline with ROT administration. This result is in harmony with the result of (Pan et al., 2020). Moreover, a significant enhancement after EMP administration was observed in TH immunoreactivity. This result is in agreement with a study on dapagliflozin (Matthews et al., 2017). TH catalyzes the rate-limiting step in dopamine synthesis, and its decline in PD is thought to be a secondary effect to dopaminergic neurons degeneration. TH may not directly function in the degeneration process due to its dopamine feedback regulation (Nagatsu et al., 2019).

Our biochemical results were supported by histopathological examination of the cerebellum, which showed a decreased number of Purkinje cells with shrunken darkly stained nuclei with dilated perineural space, which aligns with (Khadrawy et al., 2016). Purkinje cells contribute to PD pathology via loss of GABA due to necrotic changes in Purkinje cells (Khadrawy et al., 2016). These changes were prevented in EMP + ROT groups where Purkinje cells resem-

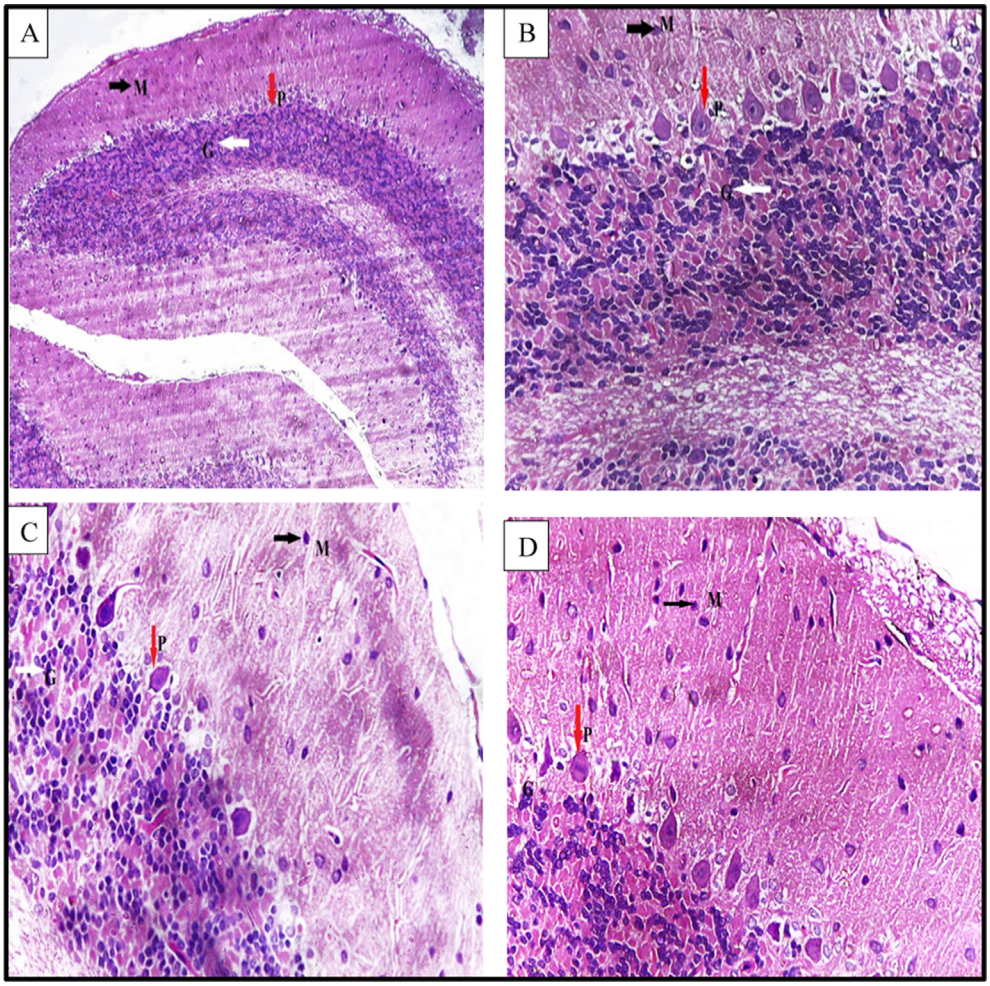

Fig. 7. A photomicrograph of a section in the cerebellar cortex of a rat **(A)**: **(control group)** showing; molecular layer (M) with few scattered cells (black arrow), Purkinje cell layer (P), Purkinje cells appear as large pyriform cells arranged in a single row (red arrows) and granular cell layer (G) appears as tightly packed small cells with deeply stained nuclei (white arrow). **(B): ROT group** showing; molecular layer (M) few scattered cells (black arrow), Purkinje cell layer (P) with deeply stained Purkinje cells with pyknotic nuclei surrounded with vacuolated neuropil (red arrows), and granular layer (G) having cells with dense nuclei white arrow. **(C): EMP1mg + ROT group** showing; molecular layer (M) few scattered cells (black arrow), Purkinje cell layer (P) few numbers of Purkinje cells with dilated perineural space (red arrows), and granular layer (G) having cells with dense nuclei white arrow. **(D): EMP2mg + ROT group** showing nearly normal molecular layer (M) with few scattered cells (black arrow), Purkinje cell layer (P), Purkinje cells appear as large pyriform cells arranged in a single row (red arrows) and granular cell layer (G) appears as tightly packed small cells with deeply stained nuclei (white arrow). ROT = Rotenone. EMP_1 = Empagliflozin 1 mg. EMP_2 = Empagliflozin 2 mg. TH = tyrosine hydroxylase.

bled those in the control group. Elfeber et al., 2004 explained this effect by the expression of SGLT mRNA in the Purkinje cells and blood vessels of brains of humans and rodents, which play a crucial role as an energy supply source for neurons on increased glucose demand, such as in hypoxemia and hypoglycemia (Sano et al., 2020).

5. Conclusion

Results of the current study revealed that, ROT administration resulted in oxidation of dopamine generating of hazardous metabolites. This is mediated by induction of oxidative stress and inflammation besides elevating MAO-B enzyme activity. Dopaminergic neuron degeneration was accelerated by overexpression of α-syn combined with downregulation of Parkin expression. EMP administration showed beneficial effects through its antioxidant potential as evidenced by restriction of oxidative stress biomarkers (MDA and NO) as well as restoration of the antioxidant mechanisms (GSH and SOD). In addition, its anti-inflammatory potential was evidenced through limitation of TNF-α and IL-1β. Preservation of the α-syn and Parkin pathways was also reported.

Declaration of Competing Interest

The authors declare that they have no known competing financial interests or personal relationships that could have appeared to influence the work reported in this paper.

Acknowledgment

The authors would like to thank Dr. Sahar Gebril, Histology Department, Faculty of Medicine, Sohag University, for assistance in fulfilling this research.

References

Abdelhamid, A.M., Elsheakh, A.R., Abdelaziz, R.R., Suddek, G.M., 2020. Empagliflozin ameliorates ethanol-induced liver injury by modulating NF-κB/Nrf-2/PPAR-γ interplay in mice. Life Sci. 256, 117908. https://doi.org/10.1016/j.lfs.2020.117908.

Abdelsalam, R.M., Safar, M.M., 2015. Neuroprotective effects of vildagliptin in rat rotenone Parkinson's disease model: role of RAGE-NF κB and Nrf2-antioxidant signaling pathways. J. Neurochem. 133 (5), 700–707. https://doi.org/10.1111/jnc.13087.

Acar, N., Parlak, H., Ozkan, A., Soylu, H., Avcı, S., Ustunel, I., Izgut-Uysal, V.N., Agar, A., 2019. The effect of docosahexaenoic acid on apelin distribution of nervous system in the experimental mouse model of Parkinson's disease. Tissue Cell 56, 41–51. https://doi.org/10.1016/j.tice.2018.12.002.

Ahmed, S.A., Mohammed, W.I., 2021. Carvedilol induces the antiapoptotic proteins Nrf2 and Bcl2 and inhibits cellular apoptosis in aluminum-induced testicular toxicity in male Wistar rats. Biomed. Pharmacother. 139, 111594. https://doi.org/10.1016/j.biopha.2021.111594.

Alabi, A.O., Ajayi, A.M., Ben-Azu, B., Bakre, A.G., Umukoro, S., 2019. Methyl jasmonate abrogates rotenone-induced parkinsonian-like symptoms through inhibition of oxidative stress, release of pro-inflammatory cytokines, and down-regulation of immnopositive cells of NF-κB and α-synuclein expressions in mice. Neurotoxicology 74, 172–183. https://doi.org/10.1016/j.neuro.2019.07.003.

Amin, E.F., Rifaai, R.A., Abdel-latif, R.G., 2020. Empagliflozin attenuates transient cerebral ischemia/reperfusion injury in hyperglycemic rats via repressing oxidative–inflammatory–apoptotic pathway. Fundam. Clin. Pharmacol. 34 (5), 548–558. https://doi.org/10.1111/fcp.12548.

Anusha, C., Sumathi, T., Joseph, L.D., 2017. Protective role of apigenin on rotenone induced rat model of Parkinson's disease: Suppression of neuroinflammation and oxidative stress mediated apoptosis. Chem. Biol. Interact. 269, 67–79. https://doi.org/10.1016/j.cbi.2017.03.016.

Arab, H.H., Safar, M.M., Shahin, N.N., 2021. Targeting ROS-Dependent AKT/GSK-3β/NF-κB and DJ-1/Nrf2 Pathways by Dapagliflozin Attenuates Neuronal Injury and Motor Dysfunction in Rotenone-Induced Parkinson's Disease Rat Model. ACS Chem. Neurosci. 12 (4), 689–703. https://doi.org/10.1021/acschemneuro.0c00722.

Balestrassi, L.S., Silva, S.M.C.A., 2021. Descriptive epidemiological study on patients with movement disorders, with emphasis on Parkinson's disease. Sao Paulo Med. J. 139, 30–37. https://doi.org/10.1590/1516-3180.2020.0119.R1.30102020.

Chakraborty, A., Diwan, A., 2019. Selection of Cells for Parkinson's Disease Cell-Therapy. Int. J. Stem Cell Res. Ther. 6, 063. https://doi.org/10.23937/2469-570X/1410063.

Chen, L., Ding, Y., Cagniard, B., Van Laar, A.D., Mortimer, A., Chi, W., Hastings, T.G., Kang, U.J., Zhuang, X., 2008. Unregulated cytosolic dopamine causes neurodegeneration associated with oxidative stress in mice. J. Neurosci. 28 (2), 425–433. https://doi.org/10.1523/JNEUROSCI.3602-07.2008.

Deng, Y., Jiang, X., Deng, X., Chen, H., Xu, J., Zhang, Z., Liu, G., Yong, Z., Yuan, C., Sun, X., Wang, C., 2020. Pioglitazone ameliorates neuronal damage after traumatic brain injury via the PPARγ/NF-κB/IL-6 signaling pathway. Genes Diseases 7 (2), 253–265. https://doi.org/10.1016/j.gendis.2019.05.002.

Dodson, M.W., Guo, M., 2007. Pink1, Parkin, DJ-1 and mitochondrial dysfunction in Parkinson's disease. Curr. Opin. Neurobiol. 17 (3), 331–337. https://doi.org/10.1016/j.conb.2007.04.010.

Elfeber, K., Stümpel, F., Gorboulev, V., Mattig, S., Deussen, A., Kaissling, B., Koepsell, H., 2004. Na+–d-glucose cotransporter in muscle capillaries increases glucose permeability. Biochem. Biophys. Res. Commun. 314 (2), 301–305. https://doi.org/10.1016/j.bbrc.2003.12.090.

Ellman, G.L., 1959. Tissue sulfhydryl groups. Arch. Biochem. Biophys. 82 (1), 70–77.

Fang, Y., Tian, X., Bai, S., Fan, J., Hou, W., Tong, H., Li, D., 2012. Autologous transplantation of adipose-derived mesenchymal stem cells ameliorates streptozotocin-induced diabetic nephropathy in rats by inhibiting oxidative stress, pro-inflammatory cytokines and the p38 MAPK signaling pathway. Int. J. Mol. Med. 30, 85–92. https://doi.org/10.3892/ijmm.2012.977.

Finch, C., Ho, S., Williams, A., Billett, E., 1995. Platelet MAO activities and MAO-B protein concentrations in Parkinson's disease and controls. In: Progress in Brain Research. Elsevier, pp. 85–90. https://doi.org/10.1016/S0079-6123(08)61205-4.

Gilda, J.E., Gomes, A.V., 2013. Stain-Free total protein staining is a superior loading control to β-actin for Western blots. Anal. Biochem. 440 (2), 186–188. https://doi.org/10.1016/j.ab.2013.05.027.

Goldstein, D.S., 2020. The catecholaldehyde hypothesis: Where MAO fits in. J. Neural Transm. 127, 169–177. https://doi.org/10.1007/s00702-019-02106-9.

Han, J.H., Oh, T.J., Lee, G., Maeng, H.J., Lee, D.H., Kim, K.M., Choi, S.H., Jang, H.C., Lee, H.S., Park, K.S., Kim, Y.-B., Lim, S., 2017. The beneficial effects of empagliflozin, an SGLT2 inhibitor, on atherosclerosis in ApoE−/− mice fed a western diet. Diabetologia 60 (2), 364–376. https://doi.org/10.1007/s00125-016-4158-2.

Hasan, R., Lasker, S., Hasan, A., Zerin, F., Zamila, M., Chowdhury, F.I., Nayan, S.I., Rahman, M.M., Khan, F., Subhan, N., Alam, M.A., 2020a. Canagliflozin attenuates isoprenaline-induced cardiac oxidative stress by stimulating multiple antioxidant and anti-inflammatory signaling pathways. Sci. Rep. 10 (1). https://doi.org/10.1038/s41598-020-71449-1.

Hasan, W., Kori, R.K., Jain, J., Yadav, R.S., Jat, D., 2020b. Neuroprotective effects of mitochondria-targeted curcumin against rotenone-induced oxidative damage in cerebellum of mice. J. Biochem. Mol. Toxicol. 34 (1). https://doi.org/10.1002/jbt.22416.

Hassanzadeh, K., Rahimmi, A., Hassanzadeh, K., 2014. Effect of N-acetylcysteine on TNF-α level of substantia nigra and striatum in rat model of Parkinson's disease. J. Mazandaran Univ. Med. Sci. 24, 40–48 http://jmums.mazums.ac.ir/article-1-4517-en.html.

Hineno, A., Kaneko, K., Yoshida, K., Ikeda, S.-I., 2011. Ceruloplasmin protects against rotenone-induced oxidative stress and neurotoxicity. Neurochem. Res. 36 (11), 2127–2135. https://doi.org/10.1007/s11064-011-0537-8.

Hoffmann, A., Ettle, B., Bruno, A., Kulinich, A., Hoffmann, A.-C., von Wittgenstein, J., Winkler, J., Xiang, W., Schlachetzki, J.C.M., 2016. Alpha-synuclein activates BV2 microglia dependent on its aggregation state. Biochem. Biophys. Res. Commun. 479 (4), 881–886. https://doi.org/10.1016/j.bbrc.2016.09.109.

Hung, Y.-F., Hsueh, Y.-P., 2021. TLR7 and IL-6 differentially regulate the effects of rotarod exercise on the transcriptomic profile and neurogenesis to influence anxiety and memory. Iscience 24 (4), 102384. https://doi.org/10.1016/j.isci.2021.102384.

Hwang, O., 2013. Role of oxidative stress in Parkinson's disease. Exp. Neurobiol. 22, 11. https://dx.doi.org/10.5607%2Fen.2013.22.1.11.

Jenner, P., Olanow, C.W., 1996. Oxidative stress and the pathogenesis of Parkinson's disease. Neurology 47, 161S–170S. https://doi.org/10.1212/WNL.47.6_Suppl_3.161S.

Jiang, H., Jiang, Q., Liu, W., Feng, J., 2006. Parkin suppresses the expression of monoamine oxidases. J. Biol. Chem. 281 (13), 8591–8599. https://doi.org/10.1074/jbc.M510926200.

Jojima, T., Tomotsune, T., Iijima, T., Akimoto, K., Suzuki, K., Aso, Y., 2016. Empagliflozin (an SGLT2 inhibitor), alone or in combination with linagliptin (a DPP-4 inhibitor), prevents steatohepatitis in a novel mouse model of non-alcoholic steatohepatitis and diabetes. Diabetol. Metabolic Syndrome 8, 1–11. https://doi.org/10.1186/s13098-016-0169-x.

Kabasakalian, P., Kalliney, S., Westcott, A., 1974. Enzymatic blood glucose determination by colorimetry of N, N-diethylaniline-4-aminoantipyrine. Clin. Chem. 20, 606–607. https://doi.org/10.1093/clinchem/20.5.606.

Kalampokini, S., Becker, A., Fassbender, K., Lyros, E., Unger, M.M., 2019. Nonpharmacological Modulation of Chronic Inflammation in Parkinson's Disease: Role of Diet Interventions. Parkinson's Disease 2019, 1–12. https://doi.org/10.1155/2019/7535472.

Kaur, H., Chauhan, S., Sandhir, R., 2011. Protective effect of lycopene on oxidative stress and cognitive decline in rotenone induced model of Parkinson's disease. Neurochem. Res. 36 (8), 1435–1443. https://doi.org/10.1007/s11064-011-0469-3.

Khadrawy, Y.A., Mourad, I.M., Mohammed, H.S., Noor, N.A., Hs, A.E., 2016. Cerebellar neurochemical and histopathological changes in rat model of Parkinson's disease induced by intrastriatal injection of rotenone. Gen. Physiol. Biophys. 36, 99–108. https://doi.org/10.4149/gpb_2016031.

Kraeuter, A.-K., Guest, P.C., Sarnyai, Z., 2019. The open field test for measuring locomotor activity and anxiety-like behavior. In: Pre-clinical Models. Springer, pp. 99–103. https://doi.org/10.1007/978-1-4939-8994-2_9.

Laczko, R., Chang, A., Watanabe, L., Petelo, M., Kahaleua, K., Bingham, J.-P., Csiszar, K., 2020. Anti-inflammatory activities of Waltheria indica extracts by modulating expression of IL-1B, TNF-α, TNFRII and NF-κB in human macrophages. Inflammopharmacology 28, 525–540. https://doi.org/10.1007/s10787-019-00658-6.

Lai, L.-L., Vethakkan, S.R., Nik Mustapha, N.R., Mahadeva, S., Chan, W.-K., 2020. Empagliflozin for the treatment of nonalcoholic steatohepatitis in patients with type 2 diabetes mellitus. Dig. Dis. Sci. 65 (2), 623–631. https://doi.org/10.1007/s10620-019-5477-1.

Li, C., Zhang, J., Xue, M., Li, X., Han, F., Liu, X., Xu, L., Lu, Y., Cheng, Y., Li, T., Yu, X., Sun, B., Chen, L., 2019. SGLT2 inhibition with empagliflozin attenuates myocardial oxidative stress and fibrosis in diabetic mice heart. Cardiovascular Diabetol. 18 (1). https://doi.org/10.1186/s12933-019-0816-2.

Li, M., Hu, J., Yuan, X., Shen, L., Zhu, L., Luo, Q., 2020. Hepcidin Decreases Rotenone-Induced α-Synuclein Accumulation via Autophagy in SH-SY5Y Cells. Front. Mol. Neurosci. 13. https://dx.doi.org/10.3389%2Ffnmol.2020.560891.

Lin, K.-J., Wang, T.-J., Chen, S.-D., Lin, K.-L., Liou, C.-W., Lan, M.-Y., Chuang, Y.-C., Chuang, J.-H., Wang, P.-W., Lee, J.-J., Wang, F.-S., Lin, H.-Y., Lin, T.-K., 2021. Two Birds One Stone: The Neuroprotective Effect of Antidiabetic Agents on Parkinson Disease—Focus on Sodium-Glucose Cotransporter 2 (SGLT2) Inhibitors. Antioxidants 10 (12), 1935. https://doi.org/10.3390/antiox10121935.

Liu, H., Hua, Y.a., Keep, R.F., Xi, G., 2019. Brain ceruloplasmin expression after experimental intracerebral hemorrhage and protection against iron-induced brain injury. Trans. Stroke Res. 10 (1), 112–119. https://doi.org/10.1007/s12975-018-0669-0.

Liu, W., Jalewa, J., Sharma, M., Li, G., Li, L., Hölscher, C., 2015. Neuroprotective effects of lixisenatide and liraglutide in the 1-methyl-4-phenyl-1, 2, 3, 6-tetrahydropyridine mouse model of Parkinson's disease. Neuroscience 303, 42–50. https://doi.org/10.1016/j.neuroscience.2015.06.054.

Machado, M.M.F., Bassani, T.B., Cóppola-Segovia, V., Moura, E.L.R., Zanata, S.M., Andreatini, R., Vital, M.A.B.F., 2019. PPAR-γ agonist pioglitazone reduces microglial proliferation and NF-κB activation in the substantia nigra in the 6-hydroxydopamine model of Parkinson's disease. Pharmacol. Rep. 71 (4), 556–564. https://doi.org/10.1016/j.pharep.2018.11.005.

Mansour, R.M., Ahmed, M.A., El-Sahar, A.E., El Sayed, N.S., 2018. Montelukast attenuates rotenone-induced microglial activation/p38 MAPK expression in rats: Possible role of its antioxidant, anti-inflammatory and antiapoptotic effects. Toxicol. Appl. Pharmacol. 358, 76–85. https://doi.org/10.1016/j.taap.2018.09.012.

Mao, Q.i., Qin, W.-Z., Zhang, A.o., Ye, N.a., 2020. Recent advances in dopaminergic strategies for the treatment of Parkinson's disease. Acta Pharmacol. Sin. 41 (4), 471–482. https://doi.org/10.1038/s41401-020-0365-y.

Marklund, S., Marklund, G., 1974. Involvement of the superoxide anion radical in the autoxidation of pyrogallol and a convenient assay for superoxide dismutase. Eur. J. Biochem. 47 (3), 469–474. https://doi.org/10.1111/j.1432-1033.1974.tb03714.x.

Matthews, V.B., Elliot, R.H., Rudnicka, C., Hricova, J., Herat, L., Schlaich, M.P., 2017. Role of the sympathetic nervous system in regulation of the sodium glucose

cotransporter 2. J. Hypertens. 35, 2059–2068. https://doi.org/10.1097/HJH.0000000000001434.
Montgomery, H., Dymock, J., 1961. Determination of nitrite in water. Analyst 86 (102), 414–416.
Montes, S., Rivera-Mancia, S., Diaz-Ruiz, A., Tristan-Lopez, L., Rios, C., 2014. Copper and copper proteins in Parkinson's disease. Oxid. Med. Cell. Longevity 2014, 1–15. https://doi.org/10.1155/2014/147251.
Nagatsu, T., Nakashima, A., Ichinose, H., Kobayashi, K., 2019. Human tyrosine hydroxylase in Parkinson's disease and in related disorders. J. Neural Transm. 126 (4), 397–409. https://doi.org/10.1007/s00702-018-1903-3.
Nakabeppu, Y., Tsuchimoto, D., Yamaguchi, H., Sakumi, K., 2007. Oxidative damage in nucleic acids and Parkinson's disease. J. Neurosci. Res. 85 (5), 919–934. https://doi.org/10.1002/jnr.21191.
Ndefo, U.A., Anidiobi, N.O., Basheer, E., Eaton, A.T., 2015. Empagliflozin (Jardiance): a novel SGLT2 inhibitor for the treatment of type-2 diabetes. Pharm. Therap. 40, 364. PMCID: PMC4450666.
Neto, J.D.N., de Almeida, A.A.C., da Silva Oliveira, J., dos Santos, P.S., de Sousa, D.P., de Freitas, R.M., 2013. Antioxidant effects of nerolidol in mice hippocampus after open field test. Neurochem. Res. 38 (9), 1861–1870. https://doi.org/10.1007/s11064-013-1092-2.
Oliveira, W.H., Nunes, A.K., França, M.E.R., Santos, L.A., Los, D.B., Rocha, S.W., Barbosa, K.P., Rodrigues, G.B., Peixoto, C.A., 2016. Effects of metformin on inflammation and short-term memory in streptozotocin-induced diabetic mice. Brain Res. 1644, 149–160. https://doi.org/10.1016/j.brainres.2016.05.013.
Pan, X., Liu, X., Zhao, H., Wu, B.o., Liu, G., 2020. Antioxidant, anti-inflammatory and neuroprotective effect of kaempferol on rotenone-induced Parkinson's disease model of rats and SH-S5Y5 cells by preventing loss of tyrosine hydroxylase. J. Funct. Foods 74, 104140. https://doi.org/10.1016/j.jff.2020.104140.
Peferoen, M., Huybrechts, R., De Loof, A., 1982. Vacuum-blotting: a new simple and efficient transfer of proteins from sodium dodecyl sulfate—polyacrylamide gels to nitrocellulose. FEBS Lett. 145, 369–372. https://doi.org/10.1016/0014-5793(82)80202-0.
Pinto, M., Nissanka, N., Moraes, C.T., 2018. Lack of Parkin anticipates the phenotype and affects mitochondrial morphology and mtDNA levels in a mouse model of Parkinson's disease. J. Neurosci. 38 (4), 1042–1053. https://doi.org/10.1523/JNEUROSCI.1384-17.2017.
Piras, F., Vecchio, D., Assogna, F., Pellicano, C., Ciullo, V., Banaj, N., Edden, R.A., Pontieri, F.E., Piras, F., Spalletta, G., 2021. Cerebellar gaba levels and cognitive interference in parkinson's disease and healthy comparators. J. Personalized Med. 11, 16. https://doi.org/10.3390/jpm11010016.
Rahimmi, A., Khosrobakhsh, F., Izadpanah, E., Moloudi, M.R., Hassanzadeh, K., 2015. N-acetylcysteine prevents rotenone-induced Parkinson's disease in rat: An investigation into the interaction of parkin and Drp1 proteins. Brain Res. Bull. 113, 34–40. https://doi.org/10.1016/j.brainresbull.2015.02.007.
Recasens, A., Dehay, B., Bové, J., Carballo-Carbajal, I., Dovero, S., Pérez-Villalba, A., Fernagut, P.-O., Blesa, J., Parent, A., Perier, C., Fariñas, I., Obeso, J.A., Bezard, E., Vila, M., 2014. Lewy body extracts from Parkinson disease brains trigger α-synuclein pathology and neurodegeneration in mice and monkeys. Ann. Neurol. 75 (3), 351–362. https://doi.org/10.1002/ana.24066.
Renshaw, A., 2006. Silverberg's Principles and Practice of Surgical Pathology and Cytopathology. LWW 13 (4), 203. https://doi.org/10.1097/00125480-200607000-00014.
Rösler, T.W., Salama, M., Shalash, A.S., Khedr, E.M., El-Tantawy, A., Fawi, G., El-Motayam, A., El-Seidy, E., El-Sherif, M., El-Gamal, M., Moharram, M., El-Kattan, M., Abdel-Naby, M., Ashour, S., Müller, U., Dempfle, A., Kuhlenbäumer, G., Höglinger, G.U., 2018. K-variant BCHE and pesticide exposure: Gene-environment interactions in a case–control study of Parkinson's disease in Egypt. Sci. Rep. 8 (1). https://doi.org/10.1038/s41598-018-35003-4.
Sano, R., Shinozaki, Y., Ohta, T., 2020. Sodium–glucose cotransporters: Functional properties and pharmaceutical potential. J. Diabetes Invest. 11 (4), 770–782. https://doi.org/10.1111/jdi.13255.
Saraf, S.L., Lin, X., Lee, G., Adjei, E.A., Kumari, N., Gordeuk, V.R., Jerebtsova, M., Nekhai, S.A., 2016. Urinary ceruloplasmin concentration predicts development of kidney disease in sickle cell disease patients. Blood 128, 4865. https://doi.org/10.1182/blood.V128.22.4865.4865.
Segura-Aguilar, J., 2017. On the role of endogenous neurotoxins and neuroprotection in Parkinson's disease. Neural Regener. Res. 12, 897. https://dx.doi.org/10.4103%2F1673-5374.208560.
Sherer, T.B., Betarbet, R., Testa, C.M., Seo, B.B., Richardson, J.R., Kim, J.H., Miller, G.W., Yagi, T., Matsuno-Yagi, A., Greenamyre, J.T., 2003. Mechanism of toxicity in rotenone models of Parkinson's disease. J. Neurosci. 23 (34), 10756–10764. https://doi.org/10.1523/JNEUROSCI.23-34-10756.2003.
Shin, S.J., Chung, S., Kim, S.J., Lee, E.-M., Yoo, Y.-H., Kim, J.-W., Ahn, Y.-B., Kim, E.-S., Moon, S.-D., Kim, M.-J., Ko, S.-H., Baek, K.-H., 2016. Effect of sodium-glucose co-transporter 2 inhibitor, dapagliflozin, on renal renin-angiotensin system in an animal model of type 2 diabetes. PLoS ONE 11 (11), e0165703. https://doi.org/10.1371/journal.pone.0165703.
Sugizaki, T., Zhu, S., Guo, G.e., Matsumoto, A., Zhao, J., Endo, M., Horiguchi, H., Morinaga, J., Tian, Z., Kadomatsu, T., Miyata, K., Itoh, H., Oike, Y., 2017. Treatment of diabetic mice with the SGLT2 inhibitor TA-1887 antagonizes diabetic cachexia and decreases mortality. NPJ Aging Mech. Disease 3 (1). https://doi.org/10.1038/s41514-017-0012-0.
Suvarna, K.S., Layton, C., Bancroft, J.D., 2018. Bancroft's theory and practice of histological techniques E-Book. Elsevier Health Sciences.
Thakur, P., Nehru, B., 2013. Anti-inflammatory properties rather than anti-oxidant capability is the major mechanism of neuroprotection by sodium salicylate in a chronic rotenone model of Parkinson's disease. Neuroscience 231, 420–431. https://doi.org/10.1016/j.neuroscience.2012.11.006.
Uchiyama, M., Mihara, M., 1978. Determination of malonaldehyde precursor in tissues by thiobarbituric acid test. Anal. Biochem. 86 (1), 271–278. https://doi.org/10.1016/0003-2697(78)90342-1.
Voss, J., Sanchez, C., Michelsen, S., Ebert, B., 2003. Rotarod studies in the rat of the GABAA receptor agonist gaboxadol: lack of ethanol potentiation and benzodiazepine cross-tolerance. Eur. J. Pharmacol. 482 (1-3), 215–222. https://doi.org/10.1016/j.ejphar.2003.10.007.
Wei, Z., Li, X., Li, X., Liu, Q., Cheng, Y., 2018. Oxidative stress in Parkinson's disease: a systematic review and meta-analysis. Front. Mol. Neurosci. 11, 236. https://doi.org/10.3389/fnmol.2018.00236.
Wu, Z., Xia, Y., Wang, Z., Su Kang, S., Lei, K., Liu, X., Jin, L., Wang, X., Cheng, L., Ye, K., 2021. C/EBPβ/δ-secretase signaling mediates Parkinson's disease pathogenesis via regulating transcription and proteolytic cleavage of α-synuclein and MAOB. Mol. Psychiatry 26 (2), 568–585. https://doi.org/10.1038/s41380-020-0687-7.
Yu, A.S., Hirayama, B.A., Timbol, G., Liu, J., Basarah, E., Kepe, V., Satyamurthy, N., Huang, S.-C., Wright, E.M., Barrio, J.R., 2010. Functional expression of SGLTs in rat brain. Am. J. Physiol.-Cell Physiol. 299 (6), C1277–C1284. https://doi.org/10.1152/ajpcell.00296.2010.
Zaitone, S.A., Ahmed, E., Elsherbiny, N.M., Mehanna, E.T., El-Kherbetawy, M.K., ElSayed, M.H., Alshareef, D.M., Moustafa, Y.M., 2019. Caffeic acid improves locomotor activity and lessens inflammatory burden in a mouse model of rotenone-induced nigral neurodegeneration: Relevance to Parkinson's disease therapy. Pharmacol. Rep. 71 (1), 32–41. https://doi.org/10.1016/j.pharep.2018.08.004.
Zhou, Z.-L., Jia, X.-B., Sun, M.-F., Zhu, Y.-L., Qiao, C.-M., Zhang, B.-P., Zhao, L.-P., Yang, Q., Cui, C., Chen, X., Shen, Y.-Q., 2019. Neuroprotection of fasting mimicking diet on MPTP-induced Parkinson's disease mice via gut microbiota and metabolites. Neurotherapeutics 16 (3), 741–760. https://doi.org/10.1007/s13311-019-00719-2.
Zinman, B., Wanner, C., Lachin, J.M., Fitchett, D., Bluhmki, E., Hantel, S., Mattheus, M., Devins, T., Johansen, O.E., Woerle, H.J., Broedl, U.C., Inzucchi, S.E., 2015. Empagliflozin, cardiovascular outcomes, and mortality in type 2 diabetes. N. Engl. J. Med. 373 (22), 2117–2128. https://doi.org/10.1056/NEJMoa1504720.